Structural, Micro-Structural and Dielectric Studies of Zirconium Doped $Ba_6Ta_4TiO_{18}$ Ceramics

Karamveer Kaur[1,*] and Anand K Tyagi[2]
[1]*Department of Physics, D M College (Panjab University) Moga, 142001 (Punjab) India.*
[2]*Department of Applied Sciences, SBS State Technical Campus, NH-05, Firozpur 152004 (Punjab) India.*

Abstract: *Zirconium doped $Ba_6Ta_4Ti_{1-x}Zr_xO_{18}$ ceramics for x= 0, 0.05, 0.1, 0.15, 0.2 and 0.25 have been successfully synthesized using auto combustion technique in this work. XRD patterns of the sintered ceramics are found to be sharp and well defined having no impurity phases for all the compositions. The lattice parameters 'a' and 'c' increase with amount of zirconium. XRD, FESEM/EDX and FTIR studies confirm the formation of $Ba_6Ta_4Ti_{1-x}Zr_xO_{18}$ ceramics with required structure. FESEM/EDX analysis revealed that ceramics possess high density with marginal inter-granular porosity. $Ba_6Ta_4Ti_{1-x}Zr_xO_{18}$ ceramic samples possess high values of dielectric constant, quality factors and conductivity. The dielectric properties enhance with increase in amount of Zirconium making them suitable for fabrication of dielectric resonators.*

Key Words: Ceramics; Sol-Gel Processes; Thermal Analysis; X-ray Diffraction; Scanning Electron Microscopy; Dielectric Properties

1. Introduction

Nowadays the advancement of microwave communication technology has increased the demand of advanced ceramics for fabrication of dielectric resonators (DRs). The ceramics used for manufacturing of DRs should have high dielectric constants, low loss factors and high thermal stability [1]. The hexagonal B site cation deficient perovskites ($A_nB_{n-1}O_{3n}$) are one of the best options as advanced ceramics. Many B site cation deficient perovskites i.e. $La_4MCrTi_3O_{15}$ (M ~ Pr, Nd and Sm) [2], $(Ba_{1-x}Mg_x)_5Nb_4O_{15}$ ($0 \leq x \leq 1$) [3], $BaLa_4Ti_4O_{15}$ [4], $Ba_3La_2Ti_2Nb_{2-x}Ta_xO_{15}$ for x = 0-2 [5], $A_6B_5O_{18}$ structures with substitution of A with Ba, Sr, La and B with Nb or Ta, Ti or Zr, and Mg or Zn [6], $Sr_5LaTi_2Nb_3O_{18}$ [7] have been reported in literature. These possess dielectric constants in the range 26-57, Q x f values in the range 2400-88000 and small values of temperature coefficient of resonant frequency and hence are the leading candidates as dielectric resonator materials. All these ceramics reported in available literature have been synthesized by high temperature solid state methods, conventional mixed oxide methods etc. The low temperature solution based techniques, which have some obvious advantages over the conventional ones, have not been employed at all for synthesis of such ceramics. The high temperature techniques offer many limitations like high consumption of energy, prone to impurities, large particle size, higher degree of agglomeration etc [8]. In comparison to this, low temperature solution techniques are easy, energy saving, pollution free, and produce contamination free, highly pure, nano size, mechanically stable and homogeneous powders at relatively low temperatures [9-10].

In this study, we have attempted the sol gel auto combustion method, a novel low temperature solution technique, to synthesize $Ba_6Ta_4TiO_{18}$ ceramics. In order to further enhance dielectric properties of synthesized ceramics, zirconium has been doped in place of titanium and $Ba_6Ta_4Ti_{1-x}Zr_xO_{18}$ ceramics for x=0, 0.05, 0.1, 0.15, 0.2 and 0.25 have been synthesized. The phase development, structure, micro-structure, morphology, elemental composition, dielectric properties i.e. quality factor, dielectric constant, conductivity etc. and effects of zirconium doping on all these properties have been investigated in detail.

2. Experimental Work

2.1 Synthesis

The low temperature synthesis of $Ba_6Ta_4Ti_{1-x}Zr_xO_{18}$ ceramics has been carried out using barium nitrate $\{Ba(NO_3)_2\}$, tantalum chloride ($TaCl_5$), titanium oxynitrate $\{TiO(NO_3)_2\}$ and zirconium oxy nitrate $\{ZrO(NO_3)_2\}$ as starting chemicals and citric acid ($C_6H_8O_7.H_2O$) as fuel. Nitric acid (HNO_3), hydrochloric acid (HCl) and ammonium hydroxide (NH_4OH) are used as solvents. In all six samples are synthesized corresponding to x=0, 0.05, 0.1, 0.15, 0.2 and 0.25 according to metallurgical reaction (1) and the obtained ceramics are referred as BTT0, BTT05, BTT1, BTT15, BTT2 and BTT25 respectively.

$$108\ Ba(NO_3)_2 + 18(1-x)TiO(NO_3)_2 + 18x\ ZrO(NO_3)_2 + 72TaCl_5 + 2214HCl + 738HNO_3 + 132C_6H_8O_7.H_2O \rightarrow 18Ba_6Ta_4Ti_{1-x}Zr_xO_{18} + 495N_2 + 792CO_2 + 2136H_2O + 1287Cl_2$$

For the synthesis of one mole of $Ba_6Ta_4Ti_{1-x}Zr_xO_{18}$, the starting chemicals barium nitrate, tantalum chloride, titanium oxynitrate, zirconium oxy nitrate and citric acid are taken in molar ratio 6: 4: 1-x: x: 7.33. An aqueous solution of Ba^{2+} cations is formed by dissolving weighed amount of $Ba(NO_3)_2$ in minimum amount of distilled water at 40°C under continuous stirring. The weighed amount of $ZrO(NO_3)_2$ is dissolved in hot water under continuous stirring to obtain an aqueous solution of Zr^{4+} cations. The solution was stirred for a maximum time of 30 minute as further heating and stirring may lead to congealing of the solution. Tantalum chloride is not soluble in water as such. It is first dissolved in aqua regia. Aqua regia is a solution having nitric acid (HNO_3) and hydrochloric acid (HCl) mixed in ratio 1:3. A mixture of nitric acid and hydrochloric acid is prepared and added to tantalum chloride under vigorous stirring at 40-50°C. Tantalum chloride is sparingly soluble in it. The solution is made clear by adding minimum amount of water [11]. It takes about 2 hours to obtain a clear solution having Ta^{5+} cations. $TiO(NO_3)_2$ solution is prepared by precipitating $Ti(OC_3H_7)_4$ in ice cold water and then dissolving the precipitate in 1.4 M HNO_3 under ice cold conditions. Above prepared aqueous Ba^{2+} solution, aqueous Zr^{4+} solution, Ta^{4+}solution and $TiO(NO_3)_2$ solution are mixed together under vigorous stirring at 50- 60°C to obtain clear solution. The citric acid solution, prepared in distilled water, is added to the above prepared solution to obtain transparent aqueous citrate-nitrate (CN) solution. Dilute ammonium hydroxide is added to (CN) solution to adjust pH to ~ 6. The obtained solution is heated at ~90°C which converts it to transparent gel due to thermal dehydration in approximately 2-3 hours. On raising the temperature the gel swells at~240°C and gets ignited with release of large amount of gaseous. It results in the formation of black voluminous powder having with little carbon residue. The obtained powder is calcined at 600°C to remove carbon residue and then pellets are prepared using Hydraulic Press. The obtained pellets are calcined at 600°C to remove binder and then sintered at 1250°C for 2 hours at heating rate of 3°C per minute. All the six samples were synthesized using the aforesaid method in a single go.

2.2 Characterization

DTA/TGA/DTG analysis of uncalcined powder is done under nitrogen atmosphere at heating rate 10°C/minute using EXSTAR TG/DTA 6300 instrument. The sintered pellets are used for X-ray diffraction analysis with the help of XPERT-PRO X-RAY diffractometer 0000000011141934 using Cu K_α radiation. SEM/EDS analysis of sintered pellets is done using using Nova Nano FE-SEM (FEI) for morphological and elemental analysis. FTIR analysis of sintered samples is carried out using FT-IR Spectrum 2 (Perkin Elmer). Dielectric properties of silver pasted pellets are measured using impedance analyzer in frequency range 100Hz to 5 MHz at room temperature.

3. Results and Discussion

3.1 Thermal Analysis

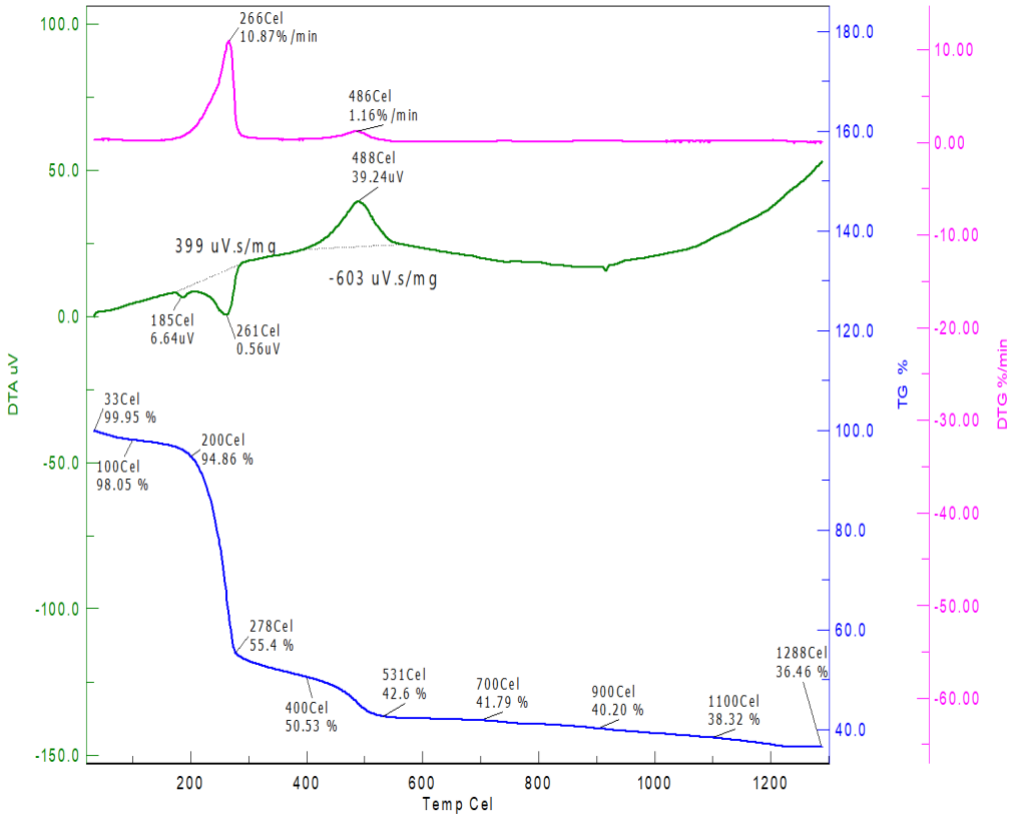

Figure 1. DTA/DTG/TG Spectrum for $Ba_6Ta_4TiO_{18}$ Uncalcined Powder

A broad endotherm up to 300°C; consisting of two endothermic peaks at 185°C and 261°C and weight loss of 45%, is observed in thermogram of undoped $Ba_6Ta_4Ti_{1-x}Zr_xO_{18}$ (x=0); BTT0 ceramic as shown in Figure 1. This may be due to loss of adsorbed moisture; trapped gases and evaporation of volatile substances. The exothermic peak observed at 488°C; with weight loss up to 7%, is due to combustion and thermal decomposition of organic substances [12]. The weight loss in temperature range from 531°C to 1288°C is about 6% with a broad endotherm up to 1200°C suggesting the onset of crystallization of the required phase.

3.2 XRD Characterization

The XRD patterns for the $Ba_6Ta_4Ti_{1-x}Zr_xO_{18}$ ($0 \leq x \leq 0.25$) ceramic samples sintered at 1250°C are given in Figure 2. All the X ray diffraction peaks are well defined and indexed with no impurity phases which indicate the purity of the synthesized samples. XRD peaks are indexed on the basis of hexagonal symmetry of the structure and are nearly similar to that of $Ba_6Nb_4TiO_{18}$ reported in the literature [6]. All the synthesized $Ba_6Ta_4Ti_{1-x}Zr_xO_{18}$ ceramic samples show almost similar XRD patterns with a shift toward the smaller angles with the increase in the amount of zirconium. This shift can be attributed to the substitution of Ti^{4+} ions; ionic radius 0.605Å by larger Zr^{4+} ions; ionic radius 0.72Å [13, 14] which leads to increase of lattice parameters.

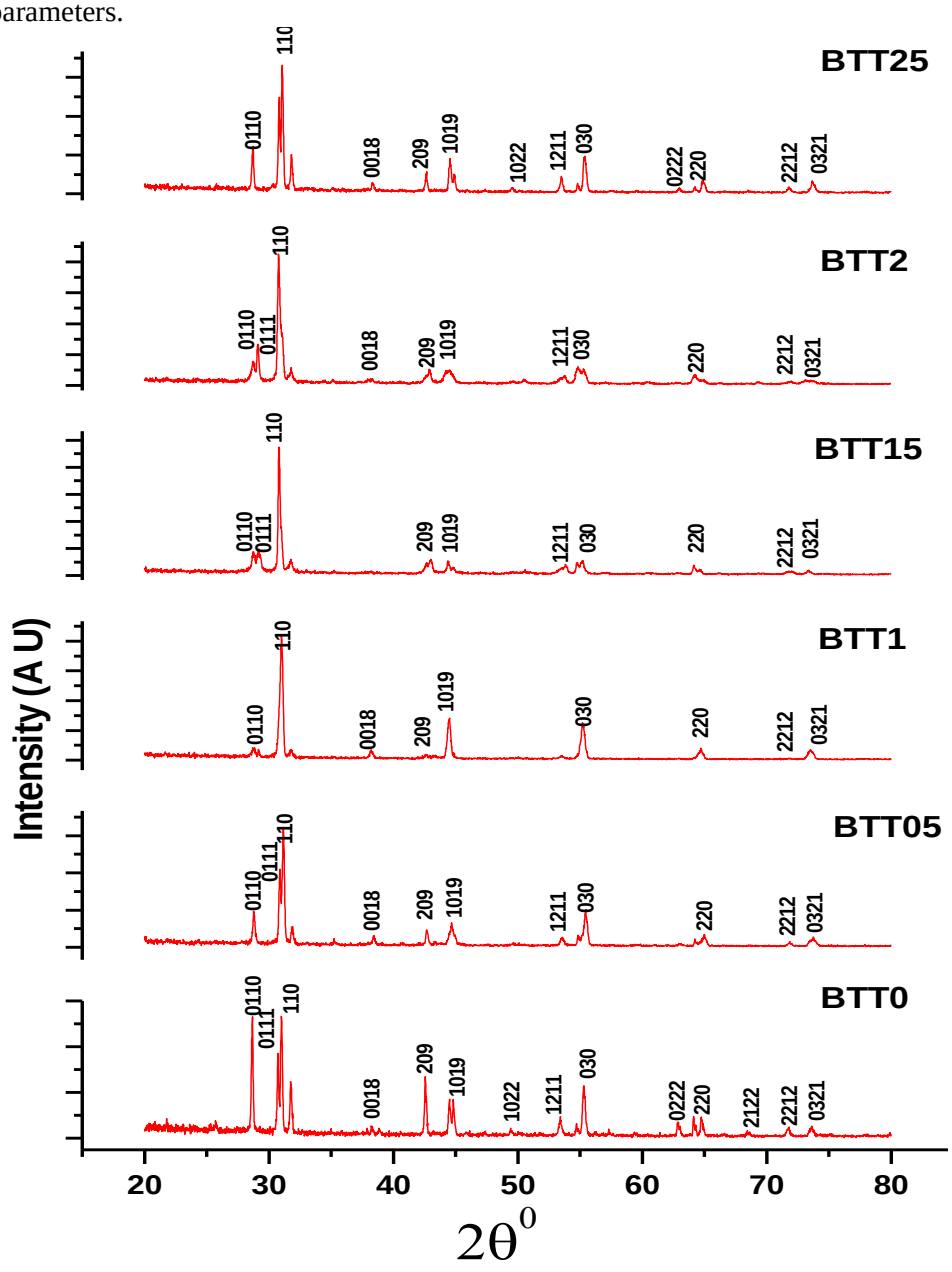

Figure 2. XRD Pattern of $Ba_6Ta_4Ti_{1-x}Zr_xO_{18}$ ($0 \leq x \leq 0.25$)

The analytical method for non cubic crystals [15] is used for indexing the XRD peaks and calculating the lattice parameters. The values of lattice parameters ('a' & 'c'), as a function of increase in the amount of Zr in $Ba_6Ta_4Ti_{1-x}Zr_xO_{18}$ ($0 \leq x \leq 0.25$), are given in the table 1.
Clearly, both the lattice parameters increase with increase in the value of x. The replacement of Ti^{4+} (0.605Å) ions by larger Zr^{4+} (0.72Å) ions results in the increase of lattice parameters of ceramics [13, 14]. Figure 3 graphically represents the variation in lattice parameters with 'x'. The decrease observed in lattice parameter 'c' at higher doping (x=0.25); in BTT25 sample may be attributed to the distortion in TiO_6 octahedral due to intake of larger Zr^{4+} ion. The crystallite sizes were calculated corresponding to XRD peaks (110), (0,1,10) and (030) for $Ba_6Ta_4Ti_{1-x}Zr_xO_{18}$ ceramic samples using Sherrer's equation [16] and was lying between 30-83 nm indicating that there is no effect of zirconium addition on crystallite size.

Table 1. Lattice Parameters for $Ba_6Ta_4Ti_{1-x}Zr_xO_{18}$ ($0 \leq x \leq 0.25$) Samples

BTT	x	a(Å)	c(Å)	c/a
BTT0	0	5.75	40.89	7.10
BTT05	0.05	5.75	41.15	7.15
BTT1	0.1	5.76	41.37	7.18
BTT15	0.15	5.77	41.62	7.21
BTT2	0.2	5.78	41.91	7.25
BTT25	0.25	5.78	41.76	7.22

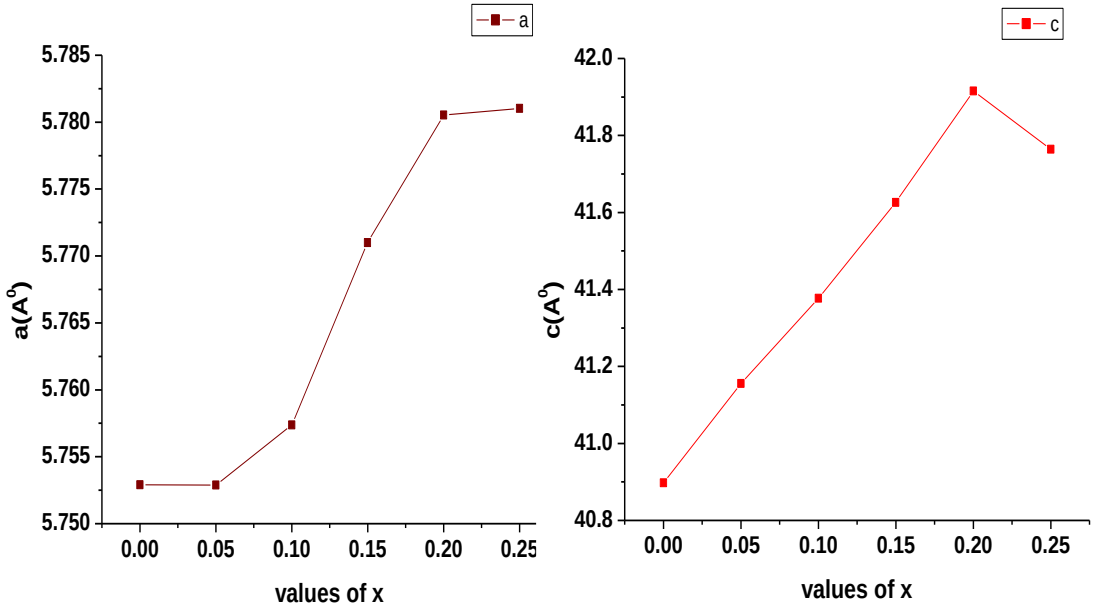

Figure 3. Variation of Lattice Parameters 'a' and 'c' with Variation in Value of x

3.3 FESEM Analysis

The microstructures of all the $Ba_6Ta_4Ti_{1-x}Zr_xO_{18}$ ceramic samples using FESEM for are shown in Figure 4. $Ba_6Ta_4Ti_{1-x}Zr_xO_{18}$ (x=0); BTT0 ceramic has bimodal distribution of grains. The grains are plate shaped and having spherical morphology. The grain boundaries are properly defined having sharp edges and corners. These ceramics show good sinterability with the small amount of inter-granular porosity and homogeneous microstructure. The grain size of x=0 sample (BTT0) lies in the range; 509 nm to 1.72 µm. The ceramic sample corresponding to x=0.05 (BTT05) possesses almost similar microstructure as that of BTT0. The microstructure is uniform, having bimodal grain distribution with plate shaped and spherical grains, well defined grain boundaries and the small amount of porosity. Size of smaller grains lies in the range from 140 nm to 434 nm and that of larger grains from 1.76 µm to 20 µm.

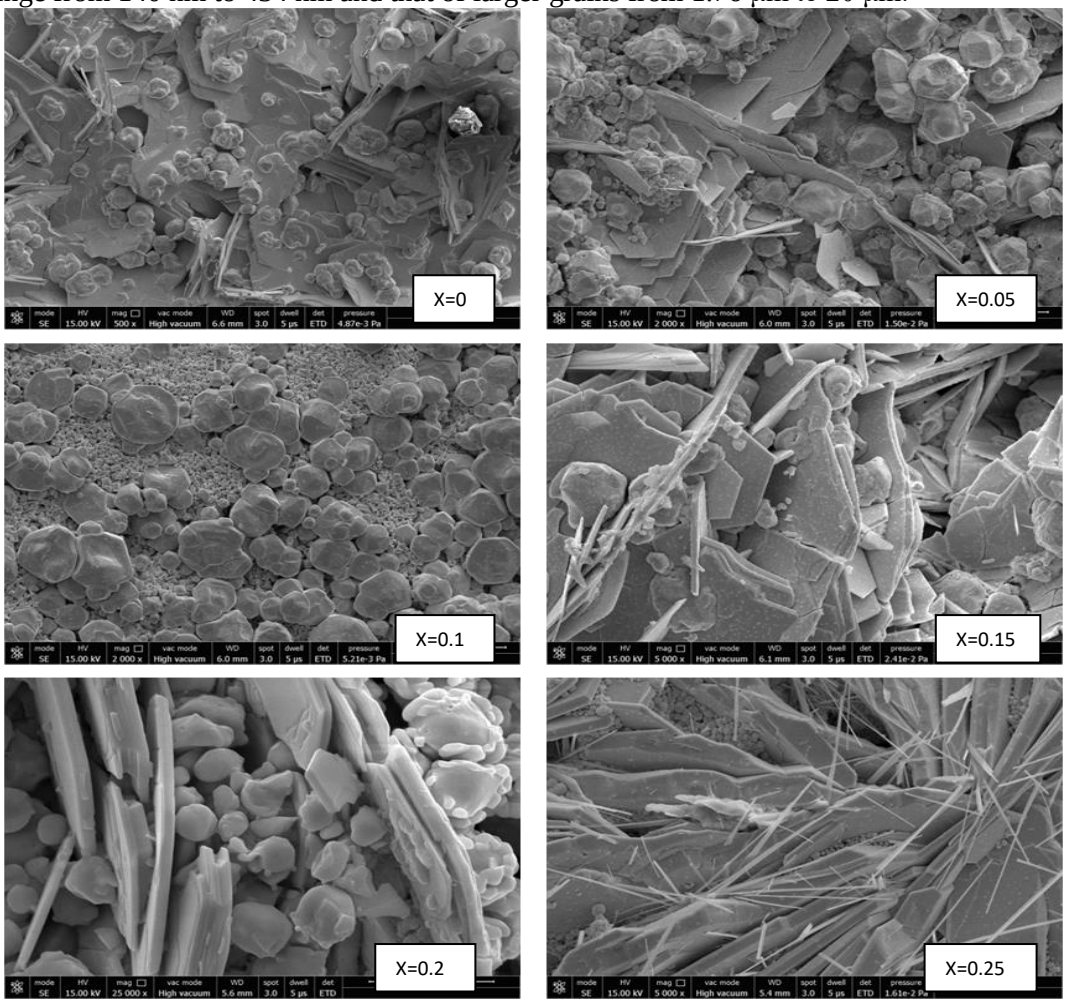

Figure 4. FESEM Images of $Ba_6Ta_4Ti_{1-x}Zr_xO_{18}$ ($0 \leq x \leq 0.25$) Ceramic Samples

$Ba_6Ta_4Ti_{1-x}Zr_xO_{18}$ (x=0.1); BTT1 ceramic has homogeneous microstructure with smaller grains in size range; 191.2 nm to 917.0 nm and the larger grains in size range; 6.2 µm to 11.8 µm. There is bimodal distribution of grains with the larger grains having polyhedral morphology and smaller grains having rod type morphology. The grain boundaries are well defined having clear edges, faces with marginal inter-granular porosity. BTT15 (x=0.15) and BTT2 (x=0.2) samples also have bimodal grain distribution having polyhedral and plate shaped grains. For

BTT15 sample, the plate shaped grains have thickness 871.7 nm and width up to 12.69 μm. There are few polyhedral grains having size range from 6.5μm to 10.20 μm. The density of this sample is found to be quite high and inter-granular porosity is reduced considerably, indicating good sinterability in this composition. BTT2 sample (x=0.2) has size range from 75.7 nm to 1.5 μm with the small amount of inter-granular porosity. BTT25 (x=0.25) sample is found to have very peculiar homogeneous microstructure with three different shapes of grains; the small sized almost spherical grains (296.8 nm to 1.5 μm), very long rod shaped grains with thickness ranging from 162.2 nm to 911.9 nm and plate shaped grain similar to that observed in BTT15 (x=0.15) sample.

It can be observed from the above description of microstructure that all the synthesized samples, except BTT25 (x=0.25) sample, have resembling microstructures. These have bimodal distribution of grains including plate shaped, rod shaped, polyhedral or spherical grains. The similar types of microstructures have been reported in literature for cation deficient perovskites ($A_nB_{n-1}O_{3n}$) [6]. The microstructure is homogeneous for all the compositions having smaller nano-metric grains and few grains with micrometers of the size. All the ceramics have small amounts of inter-granular porosity thus showing good sinterability.

3.4 EDX Analysis

From EDX (energy dispersive X ray spectra) analysis of all the BTT compositions, it was observed that only Barium, titanium, tantalum and oxygen elements are present in BTT0 sample. For all other compositions from BTT05 to BTT25, the presence of zirconium was observed along with barium, titanium, tantalum and oxygen elements. From the comparison of atomic composition obtained from EDX spectra and that calculated theoretically for $Ba_6Ta_4Ti_{1-x}Zr_xO_{18}$ ceramics, it was revealed that amounts of titanium, barium, tantalum, zirconium and oxygen are in close agreement with that calculated theoretically. In table 2, the atomic ratio of barium, titanium, tantalum, zirconium and oxygen as obtained from EDX analysis of samples is given. It can be observed that amount of zirconium goes on increasing for BTT0 to BTT25 ceramics as expected.

Table 2. Atomic Ratio of Barium, Zirconium, Titanium, Tantalum and Oxygen

Atomic ratio of Ba : Ta : Zr : Ti : O					
BTT	Ba	Ta	Zr	Ti	O
BTT0	1	0.57	0	0.31	2.6
BTT05	1	0.67	0.28	0.36	2.8
BTT1	1	0.65	0.30	0.42	2.730
BTT15	1	0.88	0.32	0.07	2.573
BTT2	1	0.58	0.33	0.18	2.023
BTT25	1	0.54	0.49	0.18	2.01

3.5 FTIR Analysis

FTIR absorption spectra for BTT0, BTT05, BTT1, BTT15 and BTT25 have been shown in the Figure 5. The absorption peak between 3459cm^{-1} to 3429 cm^{-1} for all BTT ceramics has been assigned to stretching of OH (hydroxyl) group of surface adsorbed water (H_2O).

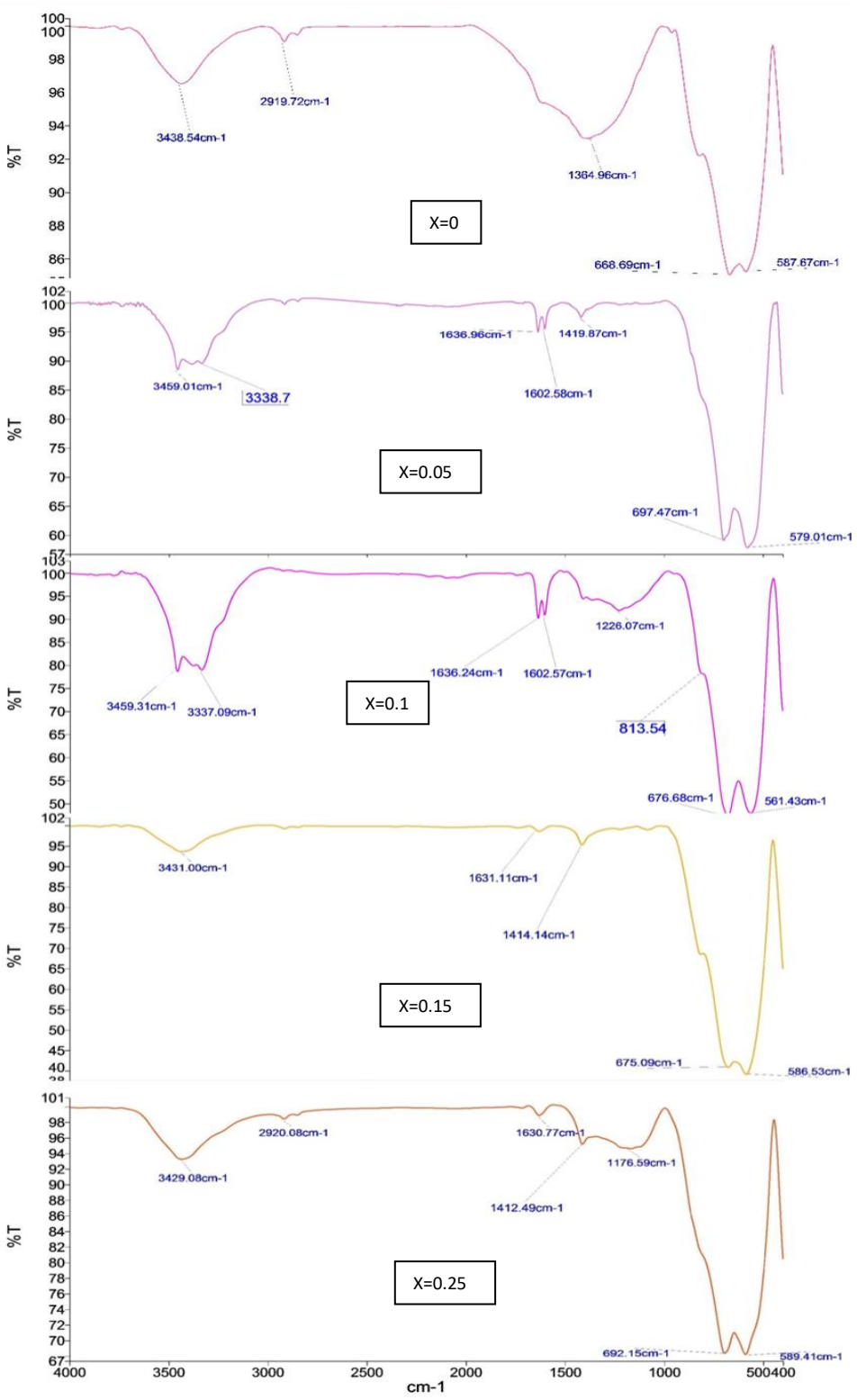

Figure 5. FTIR Spectra for $Ba_6Ta_4Ti_{1-x}Zr_xO_{18}$ ($0 \leq x \leq 0.25$)

The absorption peak with small intensity at ~ 2919.72cm^{-1} corresponds to OH bond of water molecule. The absorption peak with small intensity between 1636cm^{-1} to 1631cm^{-1} and 1412 to 1419cm^{-1} corresponds to bending mode of absorbed water (H-O-H bending) and OH bond of water molecule respectively [17, 18]. The absorption peaks at 668.69, 697.47, 676.68, 675.09 and 692.15 cm^{-1} for BTT0, BTT05, BTT1, BTT15 and BTT25 ceramics corresponds to stretching vibration of Ti-O bond [18, 19]. The absorption peaks between 589.41 to 561.43 cm^{-1} have been assigned asymmetric stretching of Ta-O bond in TaO_6 octahedral [20, 21].

Thus it can be seen FTIR spectra consist of peaks corresponding to various vibration modes of water molecule. The presence of water can be due to absorption of moisture from the environment. The presence of Ti-O bonds and Ta-O bonds in TaO_6 octahedral confirms the presence of TaO_6 octahedral which is the main part of structure of cation deficient perovskites. The face sharing and corner sharing of these TaO_6 octahedral lead to formation of hexagonal closed pack structures. The shift in wave number for Ti-O bond as 668.69, 697.47, 676.68, 675.09 and 692.15 cm^{-1} for BTT0, BTT15 and BTT25 respectively can be due to replacement of Ti^{4+} ions with Zr^{4+} ions. There is no evidence of any other peaks in the FTIR spectra.

3.6 Dielectric Characterization

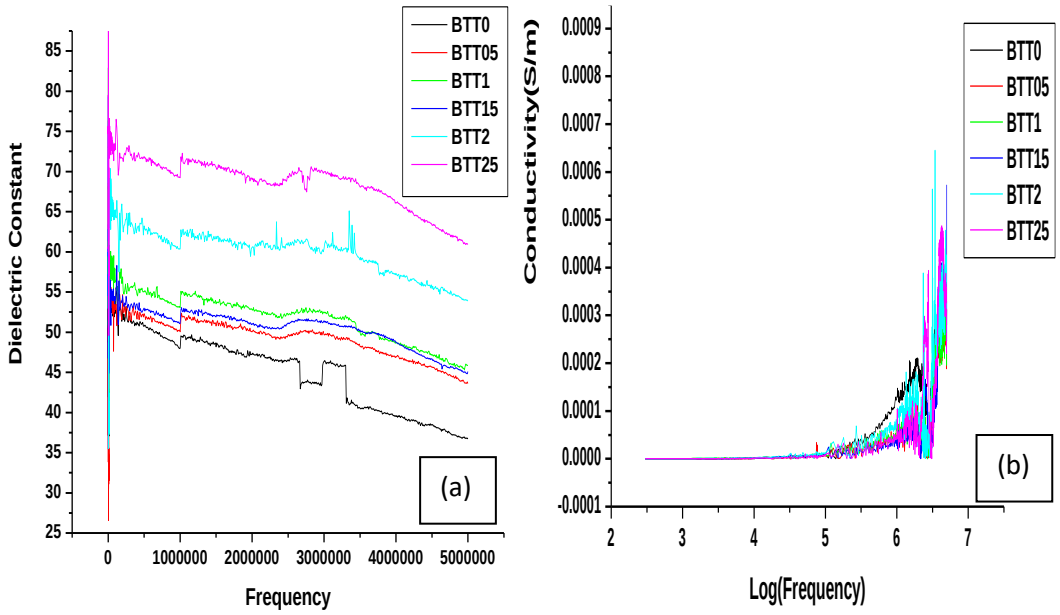

Figure 6. Variation of (a) Dielectric Constant (b) Conductivity with frequency for $Ba_6Ta_4Ti_{1-x}Zr_xO_{18}$ ceramics

The various dielectric properties i.e. dielectric constant, conductivity, quality factor etc. for all BTT ceramics are measured and their variation with frequency is analyzed. The dielectric constant values show decrease with increase of frequency (Hz) as can be seen in Figure 6(a). This is because, at low frequency contribution from electronic, ionic, orientation and space charge polarization exist but at high frequency only electronic polarization or some contribution from ionic polarization [22] is there. The dielectric constant is observed to be 58.61, 55.64, 73.088, 59.52, 74.36 & 75.53 at 1 KHz, 47.99, 50.04, 53.06, 51.09, 60.37 & 69.24 at 1 MHz and 36.84, 43.59, 45.90, 45.09, 53.88 & 60.90 at 5MHz for x =0, 0.05, 0.1, 0.15, 0.2 & 0.25 respectively. The conductivity values (Sm^{-1}) for all the compositions are almost constant at low frequencies and increase sharply at high frequencies due to the strong hopping mechanism [23]

as shown in Figure 6(b). It can be easily observed that the conductivity spectra exhibit two different regions within the measured frequency range; an intermediate plateau at low frequency and conductivity dispersion at high frequency. The intermediate plateau region corresponds to frequency independent conductivity known as DC conductivity. This region is obtained due to transport of mobile ions in response to applied electric field [24]. The maximum values of conductivity were determined to be 3.89×10^{-4} (4.8 MHz), 3.71×10^{-4}, (4.8MHz), 3.34×10^{-4} (4.83MHz), 5.73×10^{-4} (5 MHz), 6.45×10^{-4} (3.35 MHz) and 4.87×10^{-4} (4.26 MHz) Sm^{-1} for x= 0, 0.5, 0.1, 0.15, 0.2 and 0.25 respectively. The maximum values of quality factor are determined to be 25000 (2.68MHz), 3846 (2.77MHz), 25000 (2.69MHz), 20000(2.17MHz), 7692 (2.48MHz) and 25000 (2 MHz) for x = 0, 0.05, 0.1, 0.15, 0.2 and 0.25 respectively. The dielectric properties show enhancement with increase in amount of zirconium [13, 14]. The dielectric constants, quality factors and conductivity values for all the BTT ceramics are comparable to the values reported in the literature for various cation deficient perovskites ($A_6B_5O_{18}$) [6] and thus are suitable for use as dielectric material for resonators.

4. Conclusion

$Ba_6Ta_4Ti_{1-x}Zr_xO_{18}$ ceramics (x= 0, 0.05, 0.1, 0.15, 0.2 and 0.25) have been synthesized using sol gel internal combustion technique. The XRD patterns for all the compositions are sharp and well defined having no impurity phases. The lattice parameters 'a' and 'c' increase with increase in amount of zirconium. FESEM/EDX analysis revealed that ceramics obtained after sintering possess high density with marginal inter-granular porosity. The microstructure for all the Zr compositions is almost same having homogeneous distribution of grains with nano-metric and micrometer sized grains. EDX analysis suggested that the ratio of titanium, barium, tantalum, zirconium and oxygen is in close agreement with theoretical values. FTIR studies indicate the presence of TiO bonds and TaO_6 octahedral confirming the formation of $Ba_6Ta_4Ti_{1-x}Zr_xO_{18}$ ceramics with required structure. All the BTT compositions possess high values of dielectric constant, quality factors and conductivity making them suitable ceramic materials to be used for fabrication of DRs. Dielectric properties show further enhancement with increase in amount of Zirconium.

Acknowledgements

One of the authors Ms. Karamveer Kaur highly acknowledges I.K. Gujral Punjab Technical University, Kapurthala, for its valuable inputs in course of this work. The authors are also very grateful to TEQIP, MHRD/World Bank Project for providing the necessary research facilities. Furthermore, authors appreciatively acknowledge IIC, I.I.T. Roorkee, MRC, MNIT Jaipur and S B S State Technical Campus, Ferozepur for support in characterization of samples.

REFERENCES

[1] A. K. Tyagi and Parul, Procedia Materials Science, vol. 5, (2014), pp. 1322 – 1331.
[2] R. Rejini and M. Thomas, International Journal of Applied Ceramic Technology, vol. 3, no. 3, (2006), pp. 230–235.
[3] C. T. Lee, C. T. Chen, C. Y. Huang and C. J. Wang, Japanese Journal of Applied Physics, vol. 47, no. 6, (2008), pp. 4634–4637.
[4] H. Zheng, D. I. Woodward, L. Gillie and I. M. Reaney, Journal of Physics: Condensed Matter, vol. 18, (2006), pp. 7051–7062.
[5] L. Fang, Q. Yu, H. Zhang and C. Z. Hu, Material Letters, vol. 61, (2007), pp. 3093-3095.
[6] N. I. Santha and M. T. Sebastian, Journal of the American Ceramic Society, vol. 90, no. 2, (2007), pp. 496-501.

[7] H. Zhang, L. Fang, H. Su and X. Cui, Journal of Materials Science: Materials in Electronics, vol. 20, no. 8, (2009), pp. 741–744.
[8] K. I. Othman, A. H. Hassan, O. A. Abdelal et al., International Journal Engineering Science, vol.5, no. 7, (2014).
[9] S. Esposito, Materials, vol.12, (2019), pp. 668.
[10] A. Varma, A. S. Mukasyan, A. S. Rogachev, and K. V. Manukyan, Chemical Reviews, vol. 116, (2016), pp. 14493−14586. DOI: 10.1021/acs.chemrev.6b00279
[11] M. N. Ashiq, R. B. Qureshi, M. A. Malana and M. F. Ehsan, Journal of Alloys and Compounds, (2015).
[12] M. Shi, J. Zhong, R. Zuo, Y. Xu, L. Wang, H. Su and C. Gu, Journal of Alloys and Compounds, vol. 562,(2013), pp. 116–122.
[13] A. T. Oluwabi, A. O. Juma, I. O. Acik, A. Mere and M. Krunks, Proceedings of the Estonian Academy of Sciences, vol. 67, no. 2, (2018), pp. 147–157.
[14] A. Elbasset, F. Abdi, T. Lamcharfi, S. Sayouri, M. Abarkan, N. S. Echatoui and M. Aillerie, Indian Journal of Science and Technology, vol. 8, no. 13, (2015).
[15] Analytical methods for materials, crystal structure determination for non cubic crystals, laboratory module # II or http://weavegroup.ua.edu/uploads/4/8/9/48901279/lab_2__crystal_structure_determinartion_for_non_cubic_crystals.pdf
[16] A. S. Vorokh, Nanaosystems: Physics, Chemistry, Mathematics, vol. 9, no. 3, (2018), pp. 364–369. DOI 10.17586/2220-8054-2018-9-3-364-369
[17] H. Z. Akbas, Z. Aydin, I. H. Karahan, T. Dilsizoglu and S. Turgut, Proceedings of 17th Research World International Conference, Riyadh, Saudi Arabia, (2016).
[18] A. A. Aal, T. R. Hammad, M. Zawrah, I. K. Battisha and A. B. A. Hammad, Acta Physica Polonica, vol. 126, no. 6, (2014), pp. 1318-1321.
[19] L. J. Preston, M. R. M. Izawa and N. R. Banerjee, Astrobiology, vol. 11, no. 7, (2011), pp. 585-599.
[20] http://shodhganga.inflibnet.ac.in/jspui/bistream/10603/163894/11/11_chapter%203.pdf
[21] http://shodhganga.inflibnet.ac.in/jspui/bistream/10603/185868/14/14_chapter%205.pdf
[22] A. Verma, O. P. Thakur, C. Prakash, T. C. Goel and R. G. Mendiratta, Material Science and Engineering, vol. 116, no. 1, (2005).
[23] K. C. B. Naidu, T. S. Sarmash and T. Subbarao, "Synthesis and Characterization of Mn doped $SrTiO_3$ ceramics", International Journal of Engineering Research, vol. 3, no. 1, (2014).
[24] T. Badapanda, R. K. Harichandan, S. S. Nayak, A. Mishra, S. Anwar and T. Badapanda, "Frequency and temperature dependence behaviour of impedance, modulus and conductivity of $BaBi_4Ti_4O_{15}$ Aurivillius ceramic", Processing and Application of Ceramics, vol. 8, no. 3, (2014), pp. 145–153.